

- 1 Tóth, V. R., Palmer, S. C. (2016). Acclimation of *Potamogeton perfoliatus* L. to periphyton accumulation-induced
- 2 spectral changes in irradiance. *Hydrobiologia*, 766(1), 293–304.
- 3 <http://doi.org/10.1007/s10750-015-2462-3>

4 Viktor R. Tóth, Stephanie C. J. Palmer

5

6 Acclimation of *Potamogeton perfoliatus* L. to periphyton accumulation-induced spectral changes in irradiance

7

8 Balaton Limnological Institute Centre for Ecological Research Hungarian Academy of Sciences,

9 Klebelsberg K. u. 3, Tihany, Hungary, 8237

10

11 Viktor R. Tóth

12 tel: +3687448244

13 fax: +3687482006

14 toth.viktor@okologia.mta.hu

15

16 **Abstract**

17 The biomass and composition of autotrophic communities in the littoral zone are mainly affected by light
18 availability. In a field study, the spectral attenuation of periphyton was assessed. Periphyton absorbed more light
19 in the red than in the infrared spectral range, resulting in a lower red to infrared ratio (~0.3 during the most active
20 period of periphyton accumulation, compared with 0.9 to 1 otherwise). The lowest red to infrared ratio was
21 detected in the upper 20 – 40 cm of the water column. Epiphytic algae are therefore found to not only affect the
22 quantity, but also the quality of light passing through periphyton. Acclimation of *Potamogeton perfoliatus* L.
23 plantlets to such infrared-enriched light was also studied in the laboratory. During leaf morphogenesis, lower red
24 to infrared ratio light was associated with increased leaf area via the growth of existing (+85%) and the production
25 of new leaves. Intensified internode length growth (+130%) was also observed. Post-morphogenesis, no leaf or
26 internode growth was observed, new shoot production was also intensive. Leaf photochemical activity did not
27 significantly differ between groups or treatments. Results suggest that periphyton could trigger shade-tolerance
28 (leaf growth), shade-avoidance (internode growth), and morphogenetic (branch production from axillary buds)
29 adaptations in macrophytes.

30

31 **Keywords:** macrophyte; red to infrared ratio; shade-avoidance; shade-tolerance; Lake Balaton

32

33 **Introduction**

34 Light is the primary energy source for plants, affecting their growth, development and structure in both terrestrial
35 and aquatic settings, and creating strong selection pressure through its variability (Lacoul & Freedman, 2006;
36 Mooney & Ehleringer, 2009; Tilman, 2009). In the littoral zone of a turbulent lake, such as Lake Balaton,
37 submerged rooted macrophytes, growing from the sediment to the water surface with upright stems, face highly
38 variable light intensities. On a sunny day, irradiance in Lake Balaton can range over two orders of magnitude,
39 from $\sim 15 \mu\text{mol m}^{-2} \text{s}^{-1}$ at the base of a dense macrophyte stand to $\sim 1500 \mu\text{mol m}^{-2} \text{s}^{-1}$ at the water surface (Vári et
40 al., 2010; Tóth & Vári, 2013). Moreover, the change of light within a water column is spatially deterministic, thus
41 each part of the plant perceives a unique environmental signal. As highly modular organisms consisting of fairly
42 autonomous parts (i.e., leaves and connecting internodes), macrophytes are able to respond to variable irradiance
43 at the sub-individual level (de Kroon et al., 2005; Tóth & Vári, 2013). Successful adaptation by macrophytes to
44 these very different light intensities throughout the water column is possible through their modular structure, where
45 each module grow to the optimal size determined by its own optical environment resulting a greater flexibility of
46 foliar responses and thus more effective light capture (Tóth & Vári, 2013).

47 Through leaf growth, macrophytes provide a constantly increasing surface for autotrophs within the littoral zone,
48 housing a large variety of periphyton communities (Ács et al., 2005; Bécares et al., 2008; Liboriussen & Jeppesen,
49 2009; Strayer & Findlay, 2010). Greater access to light is a significant competitive advantage and macrophytes
50 employ different strategies to adapt to periphyton accumulation (Westoby et al., 2002). This constant competition
51 for light results an additional increase in spatial and temporal variability of biomass that alters the architecture of
52 individual plants, modifying the foliar morphology (Crawley, 2009; Tilman, 2009), as well as the variable species
53 density in the littoral zone of freshwater lakes (Wetzel, 1975; Kirk, 1994).

54 Macrophytes shaded by periphyton obtain significantly less light than they would in the absence of periphyton
55 growth, with the latter absorbing up to 98% of the incident light (Tóth, 2013). Adaptations to suboptimal irradiance
56 levels include vertical spread toward a more optimal light environment (shade avoidance), and the increase of leaf
57 area and the modification of photophysiological traits of plants (shade-tolerance) (Westoby et al., 2002; Valladares
58 & Niinemets, 2008; Tóth & Vári, 2013). This demonstrates that light is not only a source of energy, but also a cue
59 regarding the presence and amount of competitors.

60 Macrophyte competition with epiphytic algae results in a complex web of interactions (Vis et al., 2006; Bécares
61 et al., 2008; Tóth, 2013). Epiphytes directly influence macrophytes by decreasing the light intensity reaching the
62 leaf surface (Asaeda et al., 2004; Sultana et al., 2010; Tóth, 2013), and also absorb light preferentially in the red

63 spectral range for photosynthesis. The resulting spectral changes are detected by photoreceptors such as
64 phytochromes (Ballaré, 1999; Neff et al., 2000; Kami et al., 2010), which sense changes in irradiances between
65 300 and 780 nm (Shinomura et al., 1996) and consequently regulate the expression of genes, affecting physiology
66 and morphology, and triggering developmental changes (Neff et al., 2000; Smith, 2000; Kami et al., 2010). Studies
67 on the spectral specific effects of light on morphological and physiological properties of macrophytes have mainly
68 assessed modifications generated with regards to far red (Fr) irradiance, focusing on 730 nm in particular (Robin
69 et al., 1994; Smith & Whitelam, 1997; Whitelam & Halliday, 1999; Franklin & Whitelam, 2005) and neglecting
70 other wavelengths.

71 Signal perception initiates a set of genetic and physiological responses at the point of perception consequently
72 leading to morphological responses. This complex transduction network is a part of the intracellular signalling
73 pathway used to transmit perceived information to local genes (Quail, 2002), thus its action might be local,
74 affecting only the growth and morphogenesis of the given module. Moreover, morphological and developmental
75 modifications depend mainly on changes in cell wall properties, hence the control of plant growth and development
76 could be expected to be more pronounced during plant organ growth, morphogenesis (Kendrick & Kronenberg,
77 1994).

78 The spectral attenuation of light by periphyton (in this case the change in the red (R) to infrared (Ir) ratio, R/Ir
79 ratio, where R = 675 nm, and $700 \leq Ir \leq 800$ nm) was investigated in the mesotrophic area of Lake Balaton using
80 artificial substrates (plastic strips) throughout a full vegetation period and at different depths. It was hypothesised
81 that periphyton would alter the spectral properties of the light by preferentially absorbing in the red spectral range,
82 and therefore decreasing the R/Ir ratio. Following results from the above experiments, the effect of the R/Ir ratio
83 decrease on foliar morphology (leaf area), plant architecture (internode length) and photophysiology (electron
84 transport in PSII) of *Potamogeton perfoliatus* L. plantlets were then studied under laboratory conditions during
85 and after morphogenesis. It was hypothesised that (a) the R/Ir ratio decrease would affect both morphological and
86 physiological traits of plantlets, (b) plantlets would be more strongly affected by spectral alteration during
87 morphogenesis than in post-morphogenesis, and (c) leaves neighbouring the treated leaves would not be affected.

88

89 **Materials and Methods**

90 *In situ* experiments assessing the selective attenuation of periphyton were performed between 22 March and 9
91 October, 2010. Based on the results of these experiments, the effects of Ir-enriched radiation on plant morphology
92 and photophysiology were subsequently performed during the vegetation periods of 2011 and 2012.

93

94 *In situ periphyton experiments*

95 A site near the Balaton Limnological Institute (N: 46°54'50.53", E: 17°53'37.60") in approximately 1.4 meter deep
96 water was selected. The experimental setup was arranged 2 meters from a rocky shore, in a wave exposed area,
97 close to a *P. perfoliatus* stand. At this site, the benthic sediment is a mixture of large (30-40 cm) stones and
98 manganese rich calcite sand.

99 Plastic strips 44 mm long and 14 mm wide (~6.2 cm²), representing the average size of *P. perfoliatus* leaves on
100 the northern shore of Balaton (Vári et al., 2010; Tóth et al., 2011), were cut from APLI transparencies (Ref. 01495,
101 APLI, Spain) (for further details, see Tóth 2013). The plastic strips were attached horizontally to a vertical fishing
102 line at seven evenly distributed positions between 0 and 120 cm, with three strips at each depth. After ten days,
103 the fishing line was removed from the water and the transparency of each plastic strip was measured with a 200
104 µm diameter bifurcated fiber-optic attached to an Ocean Optics USB 2000+ spectroradiometer (Ocean Optics,
105 USA) over the range from 200 to 1100 nm. All scans were performed against a metal halide lamp and corrected
106 for the instrument's dark current. Four transparency measurements were recorded for each strip, with each
107 measurement averaging 15 separate scans. Later, each plastic strip was used for chlorophyll measurement
108 following the 90% acetone method (Ritchie, 2008). Four days after the transparency measurements, the experiment
109 was restarted with 21 new strips on a new fishing line, and was repeated every two weeks between 22 March and
110 9 October, 2010.

111

112 *Laboratory experiments*

113 Laboratory experiments were performed during the vegetation periods of 2011 and 2012, at least once a month.
114 Small, 3-10 leaved *P. perfoliatus* seedlings were collected from the shallow water area of the easternmost basin of
115 Lake Balaton immediately before each experiment. Seedlings were planted in 60 cm deep, 53 l aquaria filled with
116 5 cm of lake sediment collected from the seedling sampling area (Table 1). Water was changed at the beginning
117 of each experiment, while sediment was changed every second experiment.

118 Water and sediment characteristics were measured at the beginning of each experiment. Nitrogen (N)-forms —
119 ammonium, nitrate and urea — were determined following standard methods (Newell et al., 1967; Elliott & Porter,
120 1971; Mackereth et al., 1978). Total dissolved phosphorus (TDP) was determined after persulfate digestion (Gales
121 et al., 1966). To minimise the overall effect of thermal infrared radiation, water temperature was held constant at
122 23-24°C throughout all experiments. The tanks were illuminated by F33 Coolwhite fluorescent tubes (correlated

123 colour temperature 4000 K, Tungsram, Hungary), at $90 \mu\text{mol m}^{-2} \text{s}^{-1}$ intensity measured at the 4th leaf level with a
124 14/10 hours cycle.

125 Following one week of adaptation, four- and twelve- leaved plantlets were chosen for experiments. Plants for
126 which the fourth leaf was approximately 30% of the projected final size (estimated from previous experiments)
127 were categorized as undergoing morphogenesis, while plants for which the fourth leaf was close to (> 85%) its
128 projected final size were categorized as post-morphogenesis. In a single aquarium, 10 (5 control and 5 infrared
129 (+Ir) treatments) randomly chosen plantlets of the same size were planted. Two aquaria (morphogenesis and post-
130 morphogenesis) were simultaneously used.

131 Infrared light emitting diodes (LED; emitting irradiance: $780 \pm 14 \text{ nm}$; viewing angle: 25° ; current: 20mA) were
132 assembled into a waterproof illumination system (30 LED in a system). During the assembly of the LED
133 illumination system, the output intensity of each LED was corrected with appropriate resistors to 9mW output
134 power. In addition to the fluorescent lamps, an infrared LED was elastically attached to the fourth basal leaf of
135 every +Ir plantlet (Fig. 1). The LEDs were positioned in such a way that they did not physically interfere with
136 growth (i.e., at a small, < 2mm distance from leaf) and so that the LED could illuminate both the leaf sheath and
137 the leaf base. Based on results from the *in situ* experiments, the intensity of the infrared LED was set to a R/Ir ratio
138 of approximately 0.3-0.4 (the most frequent low R/Ir ratio resulting from the *in situ* experiments). The R/Ir ratio
139 was measured in the experimental setup without plants, using a 200 μm diameter bifurcated fiber-optic attached
140 to a spectroradiometer (USB 2000+, Ocean Optics, USA): the light of the fluorescence tubes and LED was measured
141 in the water, at the depth of the experiment (i.e., at approximately the depth of the fourth leaf). Control and treated
142 plants were kept separate from each other in different parts of the tanks. Following two weeks of illumination by
143 the infrared diodes, plants were removed from the aquaria.

144 The light response curves (i.e., the electron transport rate (ETR) of the photosystem II (PSII) as a function of
145 photosynthetically active radiation (PAR)) were measured for all leaves of all plantlets after a dark adapting period
146 of 20 minutes with a PAM-2500 (Heinz Walz GmbH, Germany). First, the ETR value was detected for a dark
147 adapted leaf with a pulse of a saturated light (630 nm, intensity $3000 \mu\text{mol m}^{-2} \text{s}^{-1}$). Later, the measured leaves
148 were exposed to 11 actinic lights (duration 15 seconds, 630 nm, intensity between 5 and $787 \mu\text{mol m}^{-2} \text{s}^{-1}$) and the
149 ETR values were measured after each illumination step with a new pulse of saturated ($3000 \mu\text{mol m}^{-2} \text{s}^{-1}$) light.
150 The light response data were fitted with the curve of Eilers and Peeters (1988), and the maximum ETR (ETR_{max}),
151 theoretical saturation light intensity (I_k) and the maximum quantum yield for whole chain electron transport (α)
152 were retrieved from this formula.

153 Each leaf was then digitalised, and leaf area (LA) was determined using ImageJ software
154 (<http://rsbweb.nih.gov/ij/>). The length of each internode was measured at the beginning and at the end of the
155 experiment.

156

157 *Mathematical and statistical data analysis*

158 Student's t-test was chosen to compare the means between treatments (control vs. +Ir). This compared the area of
159 leaves at the same leaf position at the end of the experiment and the internode growth during the 2 weeks
160 experimental period at the same internode position.

161 Leaf area at the end of the experiment was analysed by a General Linear Model (GLM) ANOVA using treatment
162 (control vs. +Ir) and morphogenetic status (during morphogenesis vs. post-morphogenesis) as categorical
163 variables, leaf position as a continuous variable, and plant number and experiment number as random variables.
164 Assumptions of normality and homoscedascity were assessed and, when necessary, raw data were transformed via
165 reciprocal transformation to obtain a normal distribution. Statistical analyses were performed in the statistical
166 software R version 2.15.3 (R Development Core Team, 2012) using the R Stats, anova and anova.glm packages.
167 Sigma Plot v 12.5 (Systat Software Inc., USA) was used to graph results and for curve fitting. Exponential rise to
168 maximum equations (Eilers & Peeters, 1988) were fitted to the light response data using the method of least
169 squares.

170

171 **Results**

172 *In situ measurements*

173 Accumulation of periphyton on the surface of the plastic strips and the preferential light absorption of chlorophyll
174 molecules (the epiphytic algae were mostly pennate diatoms; see Tóth 2013) resulted in a R/Ir ratio decrease (Fig.
175 2). The more algae were present in the periphyton, the more red light was absorbed (at around 675 nm and lower
176 than 550 nm; Fig. 3A): absorbance in the red spectral range was 40-70%, while in the Ir range, it was only 20-40%
177 (Fig. 3A). This preferential absorption resulted in a relatively higher amount of infrared radiation potentially
178 reaching the adaxial surface of the strips (i.e., a lower R/Ir ratio; Fig. 3B). Within the physiologically significant
179 Ir spectral region (i.e., 700-800 nm), the R/Ir ratio was lowest at 775 nm (Fig. 3B), while within the full infrared
180 spectrum (i.e., 700-1000 nm), the lowest R/Ir ratio was at 880 nm.

181 Based on the R/Ir ratio, two temporal groups within the vegetation period of 2010 were identified (Fig. 2A and
182 2B). The beginning of the vegetation period, from March to May, was associated with highly variable and low

183 (down to 0.17) R/Ir ratio values (Fig. 2B), while the summer-autumn period was more uniform and characterised
184 by higher mean R/Ir ratio values (Fig. 2A). In addition to the temporal pattern, a strong vertical pattern was also
185 observed, with the lowest R/Ir ratio at 20 cm below the water surface and a gradual increase with depth (Fig. 2C).
186 The decreased R/Ir ratio was attributed to periphyton accumulation. The equation ($[R/Ir]=1.049*e^{-0.001*chl-a}$) used
187 suggests that the variance of Chl-a content explained the vast majority of the R/Ir ratio variance ($R=-0.986$,
188 $P<0.001$), showing the strong and significant correlation between these variables (Pearson Product Moment
189 Correlation $R=-0.976$, $P=2.2*10^{-65}$).

190

191 *Laboratory experiments*

192 By the end of the two weeks, the smaller plantlets had an average of 7 distinguishable leaves, while the larger
193 plants grew 7 additional leaves (i.e., an average of 19 leaves). Changes in the plantlets were only observed within
194 a close vicinity of the treated leaves, and as such only the results of the 7 basal nodes are shown. During the
195 experiment, no periphyton was observed on plants, although the oldest (i.e., basal) leaves were covered by a fine
196 calcite crust.

197 Infrared treated *P. perfoliatus* plantlets showed differing growth responses depending on their morphogenetic
198 status (Figs 4 and 5, Table 2). During morphogenesis, leaf area and internode length increased: the illuminated
199 (4th) leaves were 45-80 % larger, the apically next (5th) leaves were 70-140% larger (Fig. 4A), while the leaves
200 adjacent to the illuminated leaf internodes grew longer by 90-230% (Fig. 5A). Moreover, this effect sometimes (in
201 23% of the cases) appeared on the next (5th or 6th) internodes as well (Fig. 5A, Table 2, treatment-leaf position
202 intercept: TxP). Contrary to this, the infrared illumination of the fourth basal leaf of the older plantlets that were
203 in post-morphogenesis stage had no significant effect on either leaf growth or internode length (Figs 4B and 5B).
204 During the experiment, 35% of the studied control *P. perfoliatus* plantlets produced adventitious shoots and roots,
205 while all plants illuminated with infrared irradiation grew adventitious roots and shoots (Figs 4C and 4D). The
206 produced shoots and roots of the larger plantlets (i.e., from the post-morphogenesis experiment) were longer (on
207 average 1.6 and 1.9 cm respectively) compared with the shoots and roots formed by the smaller plantlets during
208 morphogenesis (0.4 and 0.3 cm respectively) (Figs 4C and 4D).

209 Chlorophyll fluorescence showed no significant effect of infrared irradiation on the photophysiological parameters
210 of any of the *P. perfoliatus* plantlet leaves (Fig. 6). Light saturation curves of the apparent ETR of the control and
211 treated leaves were almost identical, and were not statistically distinguishable (Fig. 6A). Nevertheless, the
212 theoretical light saturation intensity (I_k) decreased as a result of the infrared radiation in the plantlets both during

213 morphogenesis and post-morphogenesis, while the maximum quantum yield for whole chain electron transport at
214 low radiation (α) slightly increased, mostly in leaves undergoing morphogenesis (Fig. 6B).

215 The GLM-ANOVA test revealed the significant effect of morphogenetic stage of the plantlets and leaf position on
216 leaf area at the end of the experiment (Table 2). Ir treatment alone was found to not have a significant effect,
217 although there was a significant interaction effect between Ir treatment and position ($P < 0.001$). In the case of
218 internode, length neither Ir treatment nor leaf position had a significant effect, while morphogenetic stage had the
219 strongest single effect on internode growth ($P = 0.023$). Although the Ir treatment alone had no effect on internode
220 growth, its interaction with internode position produced a significant ($P = 0.048$) effect (Table 2).

221

222 **Discussion**

223 *In situ measurements*

224 In addition to other factors affecting light quenching within the water column (e.g., water depth, water
225 transparency, temperature, waves, solar elevation angle, etc.), periphyton accumulation not only attenuates the
226 light reaching the leaf surface, as has previously been shown (Bécares et al., 2008; Liboriussen & Jeppesen, 2009;
227 Tóth, 2013), but also changes its spectral properties, as shown by the current results. The spectrally specific light
228 attenuation by periphyton has been found to have both a temporal and a spatial pattern. Due to the seasonal
229 difference in algal accumulation, which is not unique to Lake Balaton (Vis et al., 2007; Nõges et al., 2010), R/Ir
230 ratio was lowest in the spring months (from March to May), and, as a result of decreased periphyton biomass, was
231 close to 1 from June onward. This shift from periphyton rich to periphyton poor periods is a result of the
232 temperature dependence of pennate diatoms that comprise the majority of the epiphytic algae (Tóth, 2013). The
233 influence of temperature on algal community composition is in accordance with results from other shallow lakes
234 throughout Europe (Liboriussen & Jeppesen, 2003; Bécares et al., 2008). Parallel to this, the vertical pattern of
235 periphyton accumulation, with its maximum at 20-40 cm below the water surface, also significantly influences
236 R/Ir ratio, resulting in the lowest seasonal average ratio (~ 0.7) at this depth. Since the artificial substrate was found
237 to accumulate less periphyton than the living leaves (Tóth, 2013), it could be assumed that macrophytes might be
238 exposed to quantitatively and qualitatively distinct irradiance and consequently have to efficiently acclimate to
239 this specific light environment. The process of this acclimation and adaptation could result in the distinct vertical,
240 morphological and physiological differentiation of rooted submerged macrophytes (Barthélémy & Caraglio, 2007;
241 Mathieu et al., 2009; Tóth et al., 2011).

242 Periphyton accumulation was shown to be a crucial determinant of the R/Ir ratio. Hence, any factor influencing
243 periphyton accumulation (i.e., macrophyte biomass, leaf form and surface structure, allelopathic effect of
244 macrophytes, etc. (Zimba & Hopson, 1997; Cattaneo et al., 1998; Jones et al., 2000; Gross, 2003)) could
245 significantly influence the R/Ir ratio reaching the adaxial surface of macrophyte leaves.

246

247 *Laboratory experiments*

248 The role of far-red light has been extensively studied in the past, showing its effect on plant development (Franklin
249 & Whitelam, 2005; Franklin, 2008; Kami et al., 2010). These studies were performed predominantly on terrestrial
250 plants and demonstrate that plants grown under enriched far-red irradiance display characteristic morphological
251 changes as a response to the aboveground competition cue. The affected parameters can be grouped into shade-
252 tolerance and shade-avoidance categories (Smith & Whitelam, 1997; Franklin, 2008; Kami et al., 2010).

253 Significantly less is known about the effect of the infrared radiation on the physiology and morphology of aquatic
254 plants. In aquatic environments, spectral alteration related, for example, to self-shading that results a relative
255 increase of infrared radiation, is shown to influence the morphology of plants (Talarico & Maranzana, 2000;
256 Arenas et al., 2002; Monro & Poore, 2005). In our study of infrared radiation, we found similar results to studies
257 of far-red radiation on terrestrial plants (Ballaré, 1999; Franklin, 2008). For example, the intensification of plants'
258 vertical growth toward the surface of the water into the optimal light environment as a sign of shade-avoidance
259 (i.e., longer internodes), and simultaneous development of shade-tolerance in the form of expanded
260 photosynthetically active surface (i.e., increased leaf area) and minor photophysiological adjustments of the PSII
261 system, supporting photosynthetic performance in low light environments. These adaptations likely enhance the
262 light foraging capacity of macrophytes with dense periphyton coverage.

263 The intensive growth of adventitious tissues in *P. perfoliatus* plantlets subjected to Ir treatment was also
264 demonstrated for the first time in this study. In terrestrial plants far-red radiation promoted vertical growth (i.e.,
265 elongation) rather than horizontal expansion (i.e., branching) (Hutchings & Mogie, 1990; Kami et al., 2010).
266 Contrary to this, the 780 nm infrared enriched radiation stimulated the development of axillary buds into
267 adventitious tissues in *P. perfoliatus*, both during and after morphogenesis. This response allowed *P. perfoliatus*
268 to increase the photosynthetically active leaf area, not only via growth of already existing leaves, but also via the
269 production of new leaves from axillary buds, and thus to better forage for light.

270 Studies of phytochrome mediated responses to low R/Ir ratio do not specify the range of the effect at the plant
271 level, although suggest predominantly intracellular and not tissue level manifestation (Neff et al., 2000; Kami et

272 al., 2010). However, our results indicate a short-distance, local effect: the surplus of infrared radiation affected not
273 only the treated leaf, but also produced an effect at a limited distance of 1 module (node) (i.e., close to the
274 illuminated leaf), as has been found in terrestrial plants and for far-red radiation (730 nm, de Kroon et al., 2005).
275 These local acclimations result in a very specific vertical pattern of morphological and physiological responses
276 observed in Lake Balaton *P. perfoliatus* (Vári et al., 2010; Tóth et al., 2011; Tóth & Vári, 2013). In a vertically
277 heterogeneous light environment influenced by planktonic and epiphytic light attenuation, this higher foliar
278 variability is advantageous for *P. perfoliatus*, as it will result in a greater flexibility of responses and more effective
279 light capture by the plants.

280 This study showed that competition between epiphytic algae and its macrophyte substrate is not limited to the
281 suppression of macrophyte production via general light attenuation, as has previously been shown (Tóth, 2013).
282 Rather, epiphytic algae also change the spectral composition of light, consequently affecting leaf size and internode
283 length of *P. perfoliatus* plantlets, suggesting the involvement of phytochrome mediated hormonal and signal
284 transduction pathways (Smith, 2000; Franklin & Whitelam, 2005; Kami et al., 2010). In a broader context, our
285 results show that the importance of epiphytic algae in the transition from clear water (macrophyte governed) to
286 turbid (algae dominant) states during eutrophication (Scheffer et al., 1993; Weisner et al., 1997) might be greater
287 than was previously thought (Scheffer & Nes, 2007): the epiphytic algae growing on macrophytes could affect the
288 growth of the substrate macrophytes even in oligo-mesotrophic waters, thus under eutrophic conditions the
289 combined quantitative and qualitative effects could easily suppress the aquatic plants. Our data show that in addition
290 to the general light quenching effect of the phytoplankton and the epiphytic algae, periphyton alters the spectral
291 properties of the light reaching the adaxial surface of their substrate macrophyte leaves.

292 In conclusion, it is believed that the epiphytic communities affect the size, morphology, depth of penetration and
293 even metabolic status of their substrate species by changing the R/Ir ratio of the light. Moreover, this could further
294 affect plant architecture and the spectral properties of the water under the macrophyte canopy. However, it should
295 be noted that this study was performed on a broadleaved submerged macrophyte, and that thin-leaved and pinnate-
296 leaved species might accumulate periphyton in a different way. Furthermore, we concentrated here on the 780 nm
297 wavelength, neglecting other wavelengths. In order to obtain more generalized results and a better understanding
298 of the phenomena, comprehensive research must include macrophytes with different leaf forms and consider a
299 wider range of wavelengths between 700 and 900 nm. Such future work would provide data for improved
300 generalisation, since the effect of the periphyton on different leaf types could be expected to be very different, and
301 there is a possibility of interaction between responses triggered by irradiation at different wavelengths. Moreover,

302 at the time of intense periphyton accumulation, the quantity of light reaching the adaxial leaf surface is very
303 limited, and its quality significantly altered. Future research should also should collect information on the
304 importance of backscattered light on macrophyte production. Although the study was performed on a wide-leaved
305 species that intensively accumulate periphyton, and at 780 nm, periphyton accumulation and the consequent
306 decrease in the R/Ir ratio is likely a ubiquitous phenomenon, common to all macrophytes. In turbulent lakes, this
307 suppression of macrophyte growth by periphyton of mostly benthic origin could lead to the disappearance of
308 macrophytes from the lake, despite the low amount of planktonic algae.

309

310 **Acknowledgements**

311 This project was supported by TÁMOP-4.2.2.A-11/1/KONV-2012-0038. SCJP is grateful for the financial support
312 of GIONET, funded by the European Commission, Marie Curie Programme Initial Training Network, Grant
313 Agreement PITN-GA-2010-264509.

314

315 **References**

- 316 Ács, É., N. M. Reskóné, K. Szabó, G. Taba, & K. T. Kiss, 2005. Application of epiphytic diatoms in water
317 quality monitoring of Lake Velence-recommendations and assignments. *Acta Botanica Hungarica* 47:
318 211–223.
- 319 Arenas, F., R. M. Viejo, & C. Fernández, 2002. Density-dependent regulation in an invasive seaweed: responses
320 at plant and modular levels. *Journal of Ecology* 90: 820–829.
- 321 Asaeda, T., M. Sultana, J. Manatunge, & T. Fujino, 2004. The effect of epiphytic algae on the growth and
322 production of *Potamogeton perfoliatus* L. in two light conditions. *Environmental and experimental*
323 *botany* 52: 225–238.
- 324 Ballaré, C. L., 1999. Keeping up with the neighbours: phytochrome sensing and other signalling mechanisms.
325 *Trends in plant science* 4: 97–102.
- 326 Barthélémy, D., & Y. Caraglio, 2007. Plant architecture: a dynamic, multilevel and comprehensive approach to
327 plant form, structure and ontogeny. *Annals of Botany* 99: 375.
- 328 Bécares, E., J. Gomá, M. Fernández-Aláez, C. Fernández-Aláez, S. Romo, M. R. Miracle, A. Ståhl-Delbanco, L.
329 A. Hansson, M. Gyllström, & W. J. Van de Bund, 2008. Effects of nutrients and fish on periphyton and
330 plant biomass across a European latitudinal gradient. *Aquatic Ecology* 42: 561–574.

331 Cattaneo, A., G. Galanti, & S. Gentinetta, 1998. Epiphytic algae and macroinvertebrates on submerged and
332 floating leaved macrophytes in an Italian lake. *Freshwater Biology* 39: 725–740.

333 Crawley, M. J., 2009. *Life History and Environment Plant Ecology*. Blackwell Publishing Ltd.: 73–131,
334 <http://dx.doi.org/10.1002/9781444313642.ch4>.

335 de Kroon, H., H. Huber, J. F. Stuefer, & J. M. van Groenendael, 2005. A modular concept of phenotypic
336 plasticity in plants. *New Phytologist* 166: 73–82.

337 Eilers, P. H. C., & J. C. H. Peeters, 1988. A model for the relationship between light intensity and the rate of
338 photosynthesis in phytoplankton. *Ecological modelling* 42: 199–215.

339 Elliott, R. J., & A. G. Porter, 1971. A rapid cadmium reduction method for the determination of nitrate in bacon
340 and curing brines. *Analyst* 96: 522–527.

341 Franklin, K. A., 2008. Shade avoidance. *New Phytologist* 179: 930–944.

342 Franklin, K. A., & G. C. Whitelam, 2005. Phytochromes and shade-avoidance responses in plants. *Annals of*
343 *Botany* 96: 169–175.

344 Gales, M. E., E. C. Julian, & R. C. Kroner, 1966. Method for quantitative determination of total phosphorus in
345 water. *Journal (American Water Works Association)* 1363–1368.

346 Gross, E. M., 2003. Allelopathy of aquatic autotrophs. *Critical Reviews in Plant Sciences* 22: 313–339.

347 Hutchings, M. J., & M. Mogie, 1990. The spatial structure of clonal plants: control and consequences. *Clonal*
348 *growth in plants: regulation and function*. SPB Academic Publishing, The Hague 57: 76.

349 Jones, J. I., B. Moss, J. W. Eaton, & J. O. Young, 2000. Do submerged aquatic plants influence periphyton
350 community composition for the benefit of invertebrate mutualists?. *Freshwater Biology* 43: 591–604.

351 Kami, C., S. Lorrain, P. Hornitschek, & C. Fankhauser, 2010. Chapter Two-Light-Regulated Plant Growth and
352 Development. *Current topics in developmental biology* 91: 29–66.

353 Kendrick, R. E., & G. H. M. Kronenberg, 1994. *Photomorphogenesis in plants*. Springer.

354 Kirk, J. T. O., 1994. *Light and photosynthesis in aquatic ecosystems*. Cambridge University Press.

355 Lacoul, P., & B. Freedman, 2006. Environmental influences on aquatic plants in freshwater ecosystems.
356 *Environmental Reviews* 14: 89–136.

357 Liboriussen, L., & E. Jeppesen, 2003. Temporal dynamics in epipellic, pelagic and epiphytic algal production in a
358 clear and a turbid shallow lake. *Freshwater Biology* 48: 418–431.

359 Liboriussen, L., & E. Jeppesen, 2009. Periphyton biomass, potential production and respiration in a shallow lake
360 during winter and spring. *Hydrobiologia* 632: 201–210.

361 Mackereth, F. J. ., J. Heron, & J. F. Talling, 1978. Water analysis: some revised methods for limnologists.
362 Freshwater Biological Association, Ambleside.

363 Mathieu, A., P. H. Courn de, V. Letort, D. Barthélémy, & P. De Reffye, 2009. A dynamic model of plant growth
364 with interactions between development and functional mechanisms to study plant structural plasticity
365 related to trophic competition. *Annals of Botany* 103: 1173.

366 Monro, K., & A. G. B. Poore, 2005. Light quantity and quality induce shade-avoiding plasticity in a marine
367 macroalga. *Journal of evolutionary biology* 18: 426–435.

368 Mooney, H. A., & J. R. Ehleringer, 2009. *Photosynthesis Plant Ecology*. Blackwell Publishing Ltd.: 1–27,
369 <http://dx.doi.org/10.1002/9781444313642.ch1>.

370 Neff, M. M., C. Fankhauser, & J. Chory, 2000. Light: an indicator of time and place. *Genes & Development* 14:
371 257–271.

372 Newell, B. S., B. Morgan, & J. Cundy, 1967. The determination of urea in seawater. *J. mar. Res* 25: 201–202.

373 Nõges, T., H. Luup, & T. Feldmann, 2010. Primary production of aquatic macrophytes and their epiphytes in
374 two shallow lakes (Peipsi and Võrtsjärv) in Estonia. *Aquatic Ecology* 44: 83–92.

375 Quail, P. H., 2002. Phytochrome photosensory signalling networks. *Nature Reviews Molecular Cell Biology* 3:
376 85–93.

377 R Development Core Team, 2012. *R: A language and environment for statistical computing*. R Foundation for
378 Statistical Computing, Vienna, Austria, <http://www.R-project.org/>.

379 Ritchie, R. J., 2008. Universal chlorophyll equations for estimating chlorophylls a, b, c, and d and total
380 chlorophylls in natural assemblages of photosynthetic organisms using acetone, methanol, or ethanol
381 solvents. *Photosynthetica* 46: 115–126.

382 Robin, C. H., M. J. M. Hay, P. C. D. Newton, & D. H. Greer, 1994. Effect of light quality (red: far-red ratio) at
383 the apical bud of the main stolon on morphogenesis of *Trifolium repens* L. *Annals of Botany* 74: 119–
384 123.

385 Scheffer, M., S. Hosper, M. Meijer, B. Moss, & E. Jeppesen, 1993. Alternative equilibria in shallow lakes.
386 *Trends in Ecology & Evolution* 8: 275–279.

387 Scheffer, M., & E. Nes, 2007. Shallow lakes theory revisited: various alternative regimes driven by climate,
388 nutrients, depth and lake size. *Hydrobiologia* 584: 455–466.

389 Shinomura, T., A. Nagatani, H. Hanzawa, M. Kubota, M. Watanabe, & M. Furuya, 1996. Action spectra for
390 phytochrome A-and B-specific photoinduction of seed germination in *Arabidopsis thaliana*.
391 *Proceedings of the National Academy of Sciences* 93: 8129–8133.

392 Smith, H., 2000. Phytochromes and light signal perception by plants—an emerging synthesis. *Nature* 407: 585–
393 591.

394 Smith, H., & G. C. Whitelam, 1997. The shade avoidance syndrome: multiple responses mediated by multiple
395 phytochromes. *Plant, Cell & Environment* 20: 840–844.

396 Strayer, D. L., & S. E. Findlay, 2010. Ecology of freshwater shore zones. *Aquatic Sciences-Research Across*
397 *Boundaries* 72: 127–163.

398 Sultana, M., T. Asaeda, M. Ekram Azim, & T. Fujino, 2010. Morphological responses of a submerged
399 macrophyte to epiphyton. *Aquatic Ecology* 44: 73–81.

400 Talarico, L., & G. Maranzana, 2000. Light and adaptive responses in red macroalgae: an overview. *Journal of*
401 *Photochemistry and Photobiology B: Biology* 56: 1–11.

402 Tilman, D., 2009. *Mechanisms of Plant Competition Plant Ecology*. Blackwell Publishing Ltd.: 239–261,
403 <http://dx.doi.org/10.1002/9781444313642.ch8>.

404 Tóth, V. R., 2013. The effect of periphyton on the light environment and production of *Potamogeton perfoliatus*
405 L. in the mesotrophic basin of Lake Balaton. *Aquatic Sciences* 75: 523–534.

406 Tóth, V. R., & Á. Vári, 2013. Impact of habitat environment on *Potamogeton perfoliatus* L. morphology and its
407 within-plant variability in Lake Balaton. *Annales de Limnologie - International Journal of Limnology*
408 49: 149–155.

409 Tóth, V. R., Á. Vári, & S. Luggosi, 2011. Morphological and photosynthetic acclimation of *Potamogeton*
410 *perfoliatus* to different environments in Lake Balaton. *Oceanological and Hydrobiological Studies* 40:
411 43–51.

412 Valladares, F., & Ü. Niinemets, 2008. Shade tolerance, a key plant feature of complex nature and consequences.
413 *Annual Review of Ecology, Evolution, and Systematics* 237–257.

414 Vári, Á., V. R. Tóth, & P. Csontos, 2010. Comparing the morphology of *Potamogeton perfoliatus* L. along
415 environmental gradients in Lake Balaton (Hungary). *Annales de Limnologie-International Journal of*
416 *Limnology* 46: 111–119.

417 Vis, C., C. Hudon, & R. Carignan, 2006. Influence of the vertical structure of macrophyte stands on epiphyte
418 community metabolism. *Canadian Journal of Fisheries and Aquatic Sciences* 63: 1014–1026.

- 419 Vis, C., C. Hudon, R. Carignan, & P. Gagnon, 2007. Spatial analysis of production by macrophytes,
420 phytoplankton and epiphyton in a large river system under different water-level conditions. *Ecosystems*
421 10: 293–310.
- 422 Weisner, S. E. B., J. A. Strand, & H. Sandsten, 1997. Mechanisms regulating abundance of submerged
423 vegetation in shallow eutrophic lakes. *Oecologia* 109: 592–599.
- 424 Westoby, M., D. S. Falster, A. T. Moles, P. A. Vesk, & I. J. Wright, 2002. Plant ecological strategies: some
425 leading dimensions of variation between species. *Annual review of ecology and systematics* 125–159.
- 426 Wetzel, R. G., 1975. *Limnology*. Saunders Philadelphia.
- 427 Whitelam, G. C., & K. J. Halliday, 1999. Photomorphogenesis: Phytochrome takes a partner!. *Current biology* 9:
428 R225–R227.
- 429 Zimba, P. V., & M. S. Hopson, 1997. Quantification of epiphyte removal efficiency from submersed aquatic
430 plants. *Aquatic Botany* 58: 173–179.
- 431

432
 433 Table 1. The total dissolved nitrogen (TDN) and phosphorus (TDP) concentrations of the sediment and water
 434 during the laboratory experiments (average \pm SD, n=6).

	TDN	TDP
sediment	8093 \pm 1102 μ g l ⁻¹	150 \pm 13 μ g l ⁻¹
water	30 \pm 6 μ g l ⁻¹	14 \pm 2 μ g l ⁻¹

435

436

437 Table 2. Results of the GLM-ANOVA test of leaf area and internode growth with leaf and internode position (P)
 438 as the continuous variable, treatment (T) and morphogenetic status (M) as conditional variables.

	leaf area		internode growth	
	F Value	Pr > F	F Value	Pr > F
T	1.8	0.1811	0.1	0.768
M	652.9	<0.001	5.3	0.023
P	208.2	<0.001	1.7	0.133
T x M	0.7	0.449	0.1	0.798
T x P	49.5	<0.001	4.5	0.048
M x P	20.8	<0.001	1.9	0.081
T x M x P	0.2	0.717	0.5	0.791

439

440 Figure captions

441 Figure 1. Diagram of the laboratory experimental setup showing a *Potamogeton perfoliatus* plantlet (a.) in an
442 aquaria with the Ir LED (b.) attached the 4th leaf and the fluorescent tube (c.).

443

444 Figure 2. Seasonal (A), vertical (C) and combined (B) changes of the red/infrared ($T_{675\text{nm}}/T_{780\text{nm}}$) ratio of
445 periphyton covered plastic strips in 2010 in the mesotrophic basin of Lake Balaton. Each symbol in (A) and (C)
446 subgraphs are the average \pm SD (n = 21 and 42, respectively); (B) shows averages.

447

448 Figure 3. The effect of periphyton chl-a concentration on the transparency of the experimental plastic strips in
449 the range between 340 to 1000 nm (A) and the ratio of transparency at 675 nm to the transparency shown on the
450 x axis ($T_{675\text{nm}}/T_i$) (B). Clear plastic strips are represented by bold solid lines, while plastic strips covered with
451 increasing amounts of periphyton (and higher chl-a concentration) are represented by green and brown lines.
452 Each line is an average of 60 measurements.

453

454 Figure 4. Leaf area (LA – figures A, B), and length of adventitious shoots (figures C, D, upper part) and roots
455 (figures C, D, lower part) at the end of the experiment in plantlets during leaf morphogenesis (A, C) and after
456 leaf morphogenesis (B, D). Control treatments are represented by white symbols and bars, while infrared
457 irradiated plants (+Ir) are represented by black symbols and bars. The fourth basal leaf of each +Ir treatment was
458 irradiated with infrared light (leaf #1 is the most basal). Each symbol represents the average \pm SD (n = 5).
459 Treatments at each leaf position were compared through a t-test; * is a significant difference at $P < 0.05$.

460

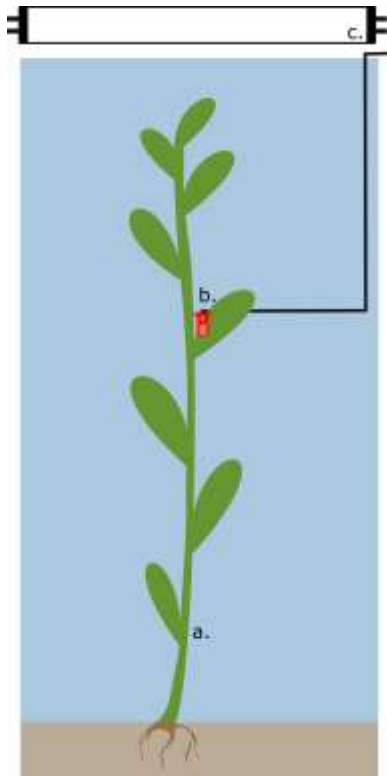
461 Figure 5. Change of internode growth (RG, cm cm^{-1}) during leaf morphogenesis (A) and after leaf
462 morphogenesis (B). Control treatments are represented by white symbols, infrared irradiated plants (+Ir) are
463 represented by black symbols. The fourth basal leaf of each +Ir treatment was irradiated with infrared light
464 (internode #1 is the most basal). Each symbol represents the average \pm SD (n = 5). Treatments at each leaf
465 position were compared through a t-test; * is a significant difference at $P < 0.05$.

466

467 Figure 6. Photophysiological properties of *Potamogeton perfoliatus* leaves. A: Light saturation curve of the
468 apparent electron transport rate (ETR) of the 4th leaves of the control (squares) and infrared irradiated plants (+Ir;
469 circles) of plantlets during (black symbols) and after (white symbols) morphogenesis. All fits resulted in $R > 0.99$.

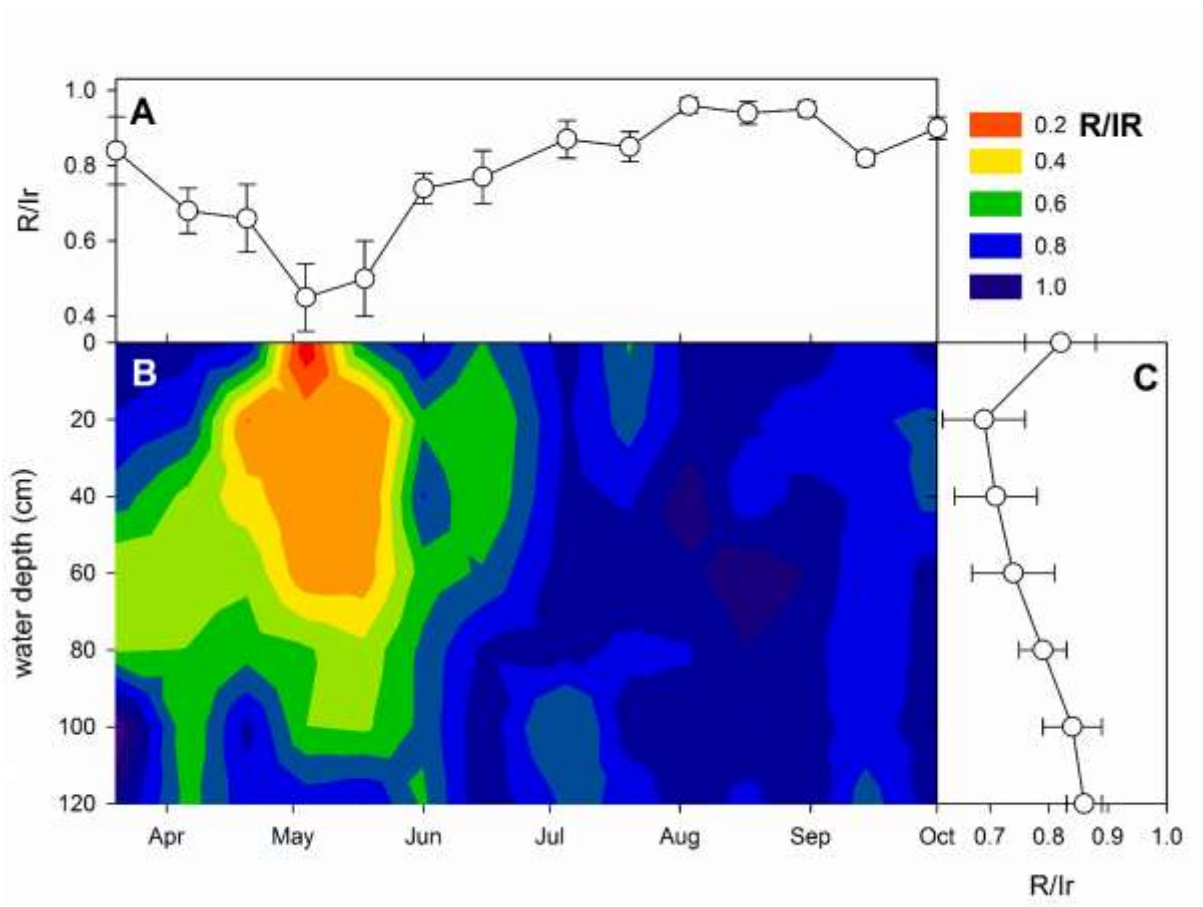
470 **B:** The maximum electron transport capacity (ETR_{max}), the theoretical light saturation intensity (I_k) and the
471 maximum quantum yield for whole chain electron transport (α) of the infrared irradiated plantlets during (black
472 bars) and after (white bars) morphogenesis. The fourth leaf of +Ir treatment were irradiated with far-red light
473 (leaf #2 is second to the basal leaf).

474



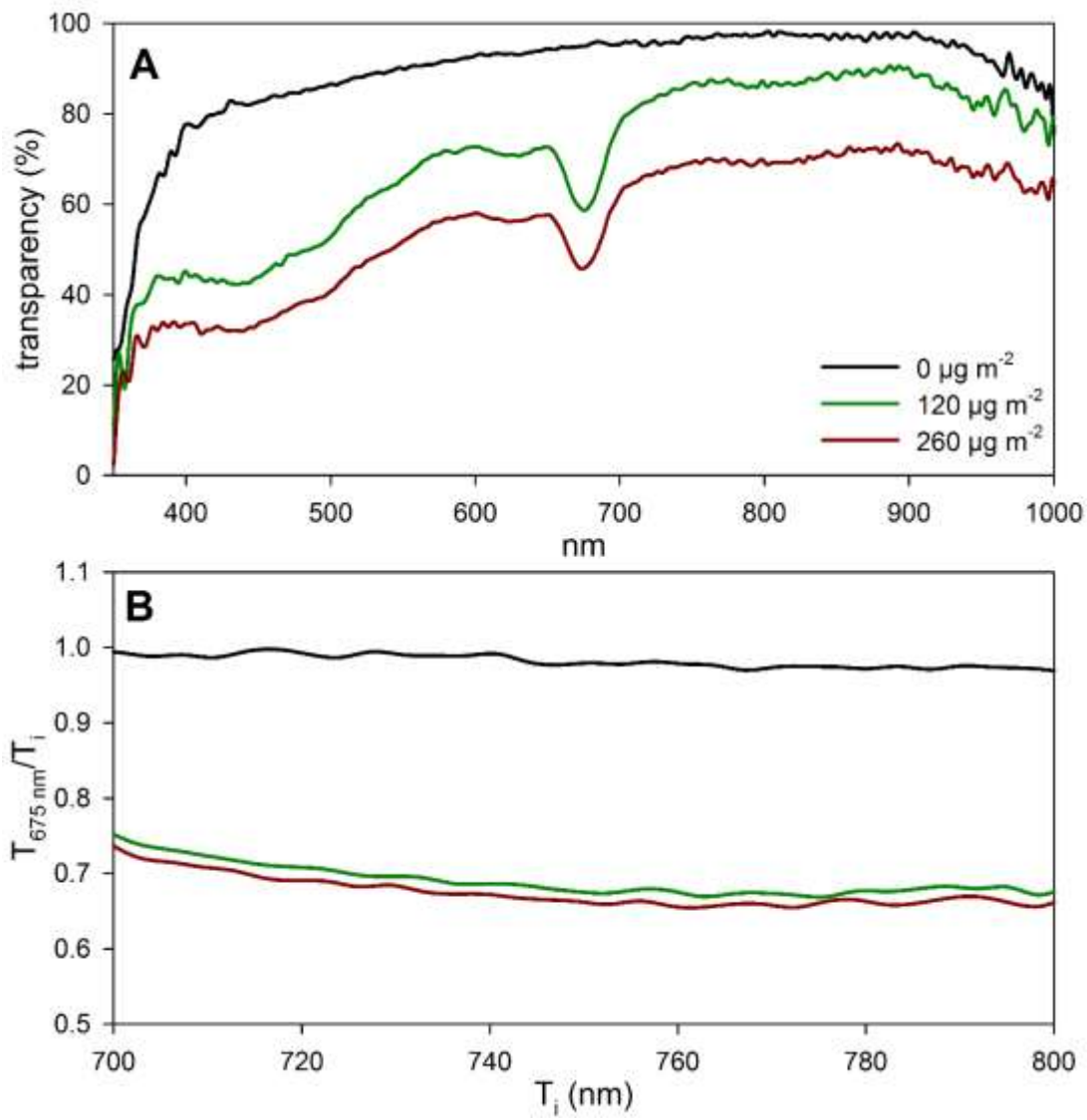
475

476 Fig. 1.



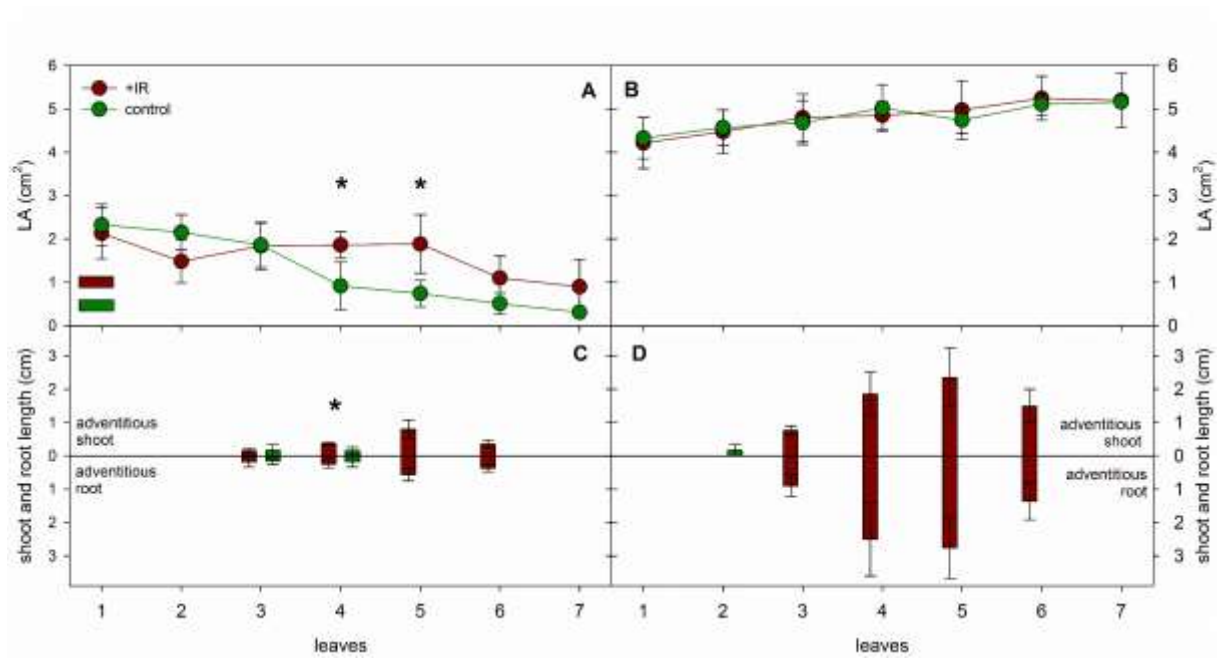
477

478 Fig. 2.



479

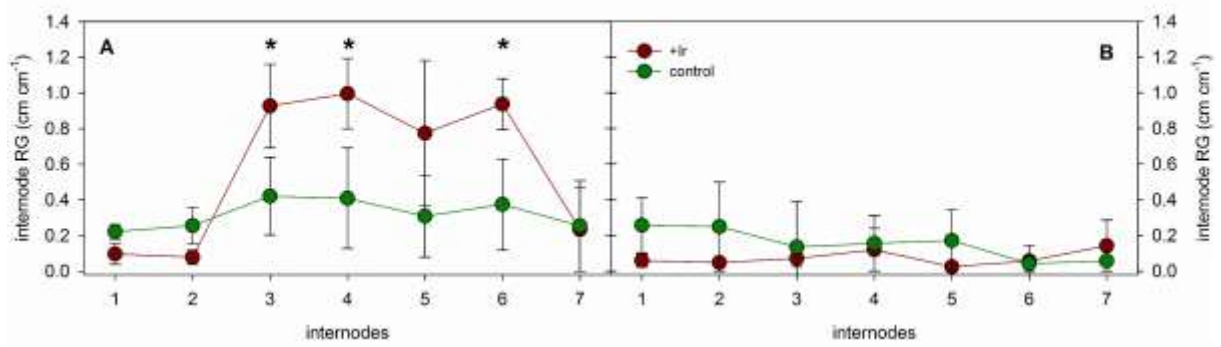
480 Fig. 3.



481

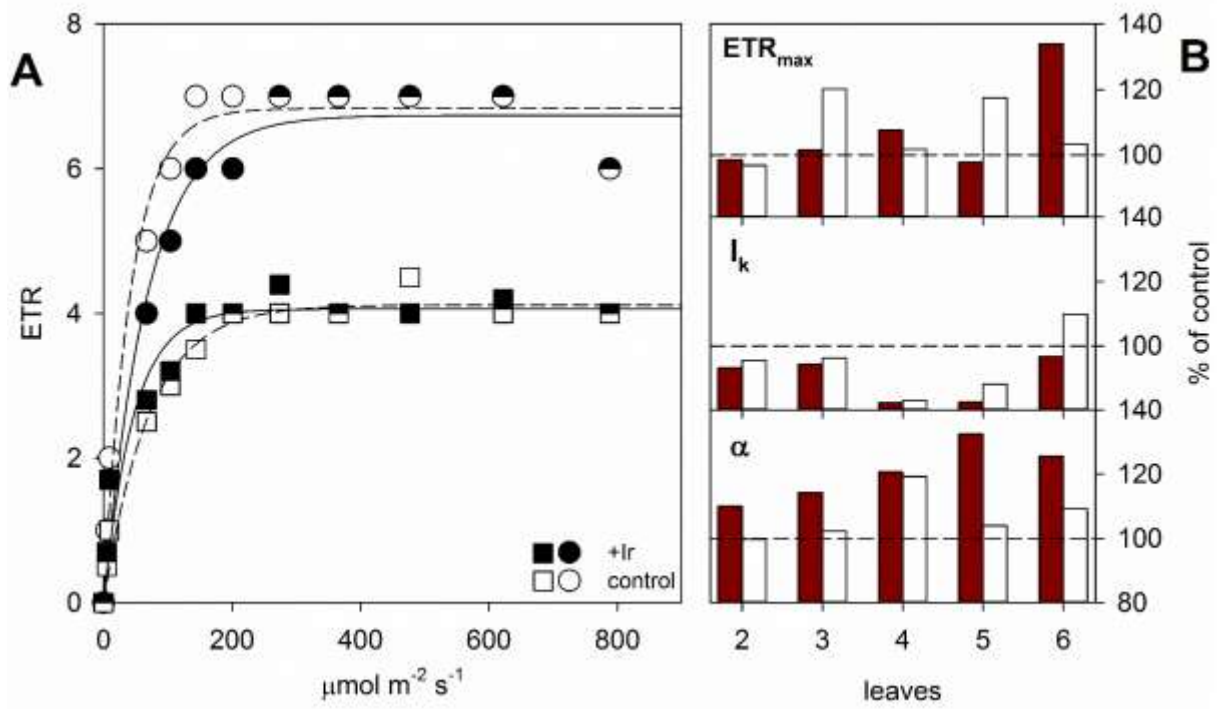
482 Fig. 4.

483



484

485 Fig. 5.



486

487 Fig. 6.